Asian Pub. Corp.

www.asianpubs.org

ARTICLE

Phase Diagram, Thermodynamic Stability and Interfacial Studies on Solid Dispersions of Phenothiazine-Acetanilide Drug System

H. Shekhar✉ and Manoj Kumar

Asian Journal of Organic & Medicinal Chemistry

Volume: 1 Year: 2016
Issue: 1 Month: January-March
pp: 26-32
DOI: http://dx.doi.org/10.14233/ajomc.2016.AJOMC-P12

Received: 9 April 2016
Accepted: 25 April 2016
Published: 10 May 2016

ABSTRACT

The study of solid liquid dispersions of binary drug system has been very useful in providing the significant enhanced pharmaceutical properties as compared to the parent drug. The present communication includes the thermodynamic and interfacial investigation of phenothiazine and acetanilide binary eutectic and non-eutectic drug dispersions. Simple eutectic dispersion was observed at 0.855 mole fraction of acetanilide at melting temperature 108 °C. Partial and integral thermodynamic quantities such as, excess Gibbs energy (g^E), excess enthalpy (h^E), excess entropy (s^E) of eutectic and non-eutectic mixtures were also calculated using activity coefficient data. The value of excess Gibbs free energy indicates positive deviation from ideal behaviour which refers stronger association between like molecules during formation of binary mixture. However, the negative value of mixing function, Gibbs free energy of mixing (ΔG^M) suggests the mixing for eutectic and non-eutectic is spontaneous. The interfacial properties such as entropy of fusion per unit volume (ΔS_v), interfacial energy (σ), roughness parameter (α), grain boundary energy of parent components, eutectics and non-eutectics have been studied using enthalpy of fusion data. Gibbs-Thomson coefficient evaluated by numerical method is also very helpful to compute the interfacial energy. The size of critical nucleus at different undercoolings has been found in nanoscale, which is itself a big challenge in pharma-ceutical world. The value of $\alpha > 2$, suggests the irregular and faceted growth proceeds in binary alloys.

KEYWORDS

Phase diagram, Thermodynamic and mixing functions, Thermal stability, Critical radius, Interfacial energy, Microstructure.

INTRODUCTION

Phenothiazine is a bioactive heterocyclic compound having extensive pharmaceutical applications *viz*. antibacterial [1], antifungal [2], antitubercular [3], antischizophrenics [4] and anti-inflammatory [5]. The compound is related to the thiamine-class of heterocyclic compound and its derivatives find wide use as drugs. The most widely used phenothiazine skeleton is chlorpromazine and is prescribed for overactive schizophrenics; trifluoperazine which is used for inhibited and withdrawn schizophrenics. Phenothiazine derivatives have also been used for anaesthesia and to control itching. Although

Author affiliations:

Department of Chemistry, V.K.S. University, Ara-802 301, India

✉To whom correspondence to be addressed:

E-mail: hshe2503@rediffmail.com

Available online at: http://ajomc.asianpubs.org

many patients on intake of phenothiazine derivatives and other narcoleptics show marked improvement, these drugs on consumption over long periods of time become fairly toxic. A number of substituted phenothiazines were synthesized and screened for biological activity against the regulatory enzymes involved in allergic disease. The activity of phenothiazine derivatives *e.g.*, promethazine, levomepro, prochlorperazine, fluphenazine and thioridazine and their potential for the therapy of problematic infections [6] against protozoa, parasites, antimicrobial effects have been highlighted earlier. Phenothiazines inhibit ABC type efflus pumps that responed for the antibiotic resistance of many micro-organism [7]. They also inhibit calcium binding to calmodulion type proteins of the calcium channel verapamil. On the second hand acetanilide was utilized as an alternative to aspirin to treat various ailments. It was first used in medical practice as Antifebrin in 1886 for its fever reduction and pain killing properties. It has been treated for the production of 4-acetamidobenzenesulphonyl chloride, a key intermediate for the manufacture of sulpha drugs. It has been a good precursor in synthesis of pencillin and other pharmaceuticals and their intermediates. The quantum of toxicity and analgesic potency [8] have also been discussed in terms of the variety of substituents to the ring of acetanilialide. The structure effect of a series of substituted acetanilide in antimicrobial activity against *S. aureus*, *E. coli* and *C. albicans* was also studied. Acetanilide based compounds, 2-pyridylacetanilide, pyrimidin – 2-ylacetanilide and pyrazin-2-ylacetanilide have recently been reported as potential drugs in form of potent and selective beta3-adrenergic receptor (AR) agonists for the treatment of obesity and non-insulin-dependent (type11) diabetes. However, no longer and direct use of acetanilide is suggested due to causing methemoglobinemia in which excess metheglobin does not enact function reversibly as an oxygen carrier in the blood. Due to the most alarming, being cyanonise and unacceptable toxic effects of aniline a hydrolyzed product of acetanilide in the body, a successful and less toxic antipyretic and analgesic metabolite paracetamol (4'-hydroxyacetanilide/ acetaminophen) is now preferred and widely used. In addition in the 19th century it was very significant compound used as experimental photographic developers. It works as safe guard and inhibitor with hydrogen peroxide for stabilizing cellulose ester varnishes. It is also used as an intermediate for the synthesis of rubber accelerator, dyes and its intermediate and camphor synthesis.

During last few years the solid dispersion of binary pharmaceutical systems [9-11] are being used as model system for studying the rapid growth of nanoparticles with controlled microstructures with point view to get desired physical, chemical and medicinal properties of solid dispersions. The kinetic, themodynamic and interfacial investigation of these dispersions can also be understood to a great extent which may very significant for deciding their efficacy and bio applicability. Having wide spread biological and pharmacological applications of phenothiazine (PT) and acetanilide (ACT), PT-ACT binary system may have better future and hopes in developing and designing of the virgin and new binary drugs. In recent years pharmaceutical properties of eutectic and non-eutectic solid dispersions of binary drug systems have been reported with increase the solubility, dissolution rate, hygroscopicity and chemical stability. Keeping the view of better pharmacological performance and efficacy of binary product of PT-ACT system, it is aimed to investigate the properties of binary drug dispersions in the solid state emphasizing thermodynamic and interfacial studies, such as phase diagram, excess and mixing thermodynamic functions, activity and activity coefficient, thermal stability, interfacial energy, surface roughness, driving force of solidification and critical radius.

EXPERIMENTAL

Phenothiazines (Sigma, India) and acetanilide were directly taken for investigation. The melting point of phenothiazines was found 189 °C while for acetanilide it was found 115 °C. For measuring the solid-liquid equilibrium data of PT-ACT system, mixtures of different compositions of both were made in glass test tubes by repeated heating and followed by chilling in ice and melting temperatures of solid dispersions were determined by the Thaw-Melt method [12]. The melting and thaw temperatures were measured by a Toshniwal melting point apparatus with help of a precision thermometer which could read correctly up to ± 0.1 °C. The heater was regulated to increase by 1 °C in temperature in every 5 min. The value of enthalpy of fusion of phenothiazine and acetanilide was measured by the DTA method using NETZSCH Simultaneous Thermal Analyzer, STA 409 series unit.

RESULTS AND DISCUSSION

Phase diagram study: The solid liquid equilibrium (SLE) data of PT-ACT system determined by the thaw melt method is reported in Table-1. The system shows the formation of a eutectic (Fig. 1), which has a minimum melting temperature, *i.e.* a eutectic point. The eutectic point of a binary condensed mixture is defined as the temperature at which a solid mixture phase is in equilibrium with the liquid phase and a eutectic is generally considered to be a simple mechanical mixture of the solid and liquid [13]. The thaw temperature is the temperature at which the first droplet of liquid appears in a mixture-containing capillary. The liquidus temperature is the maximum temperature at which both solid crystals and liquid are observed to coexist. Above this temperature, there is only liquid phase present. The melting point of phenothiazine (189 °C) decreases on the addition of second component acetanilide (m.p., 116 °C) and further attains minimum and then increases. Eutectic E (0.372 mole fraction of phenothiazine) is obtained at 143 °C. At the eutectic temperature a liquid phase L and two solid phases (S_1 and S_2) are in equilibrium and the system is invariant. The homogenous binary liquid solution exists in the region above the eutectic temperature while the two solid phases exists in the region below the eutectic temperature. The region located below the liquidus line on the left side a binary liquid and solid phenothiazine exist while in a similar region located on the right side a binary liquid and solid acetanilide system co-exist.

$$L \underset{}{\overset{\text{Cooling}}{\rightleftharpoons}} S_1 + S_2$$

TABLE-1
PHASE COMPOSITION, MELTING TEMPERATURE, VALUES OF ENTROPY OF FUSION PER UNIT VOLUME (ΔS_v), HEAT OF FUSION (ΔH), INTERFACIAL ENERGY (σ), GRAIN BOUNDARY ENERGY (σ_{gb}), GIBBS-THOMSON COEFFICIENT (τ) AND ROUGHNESS PARAMETER (α)

Alloy	χ_{PT}	m.p. (°C)	ΔH (J/mol)	ΔS (J/mol/K)	α	$\sigma \times 10^{-2}$ (J/m^2)	$\sigma_{gb} \times 10^2$ (J/m^2)	ΔS_V (kJ/m^3/K)	ΔH_V	$\tau \times 10^6$ Km
A_1	0.070	111	22275.10	58.01	6.98	3.69	7.14	507.1	194.74	7.28
E	0.145	108	22547.74	59.18	7.12	3.68	7.12	506.0	192.79	7.28
A_2	0.225	114	22839.80	59.02	7.10	3.67	7.10	493.0	190.79	7.45
A_3	0.311	132	23153.43	57.17	6.88	3.66	7.08	466.0	188.75	7.86
A_4	0.404	145	23491.11	56.20	6.76	3.66	7.06	446.5	186.65	8.19
A_5	0.504	147	23855.71	56.80	6.83	3.65	7.04	439.3	184.51	8.30
A_6	0.613	165	24250.59	55.37	6.66	3.64	7.03	416.2	182.31	8.74
A_7	0.731	172	24679.69	55.46	6.67	3.63	7.01	404.6	180.06	8.97
A_8	0.859	178	25147.65	55.76	6.71	3.62	6.99	394.1	177.75	9.18
Phenothiazines	–	189	25660.00	55.54	6.68	3.61	6.98	379.6	175.38	9.51
Acetanilide	–	115	22020.00	56.75	6.83	3.70	7.15	506.8	196.64	7.31

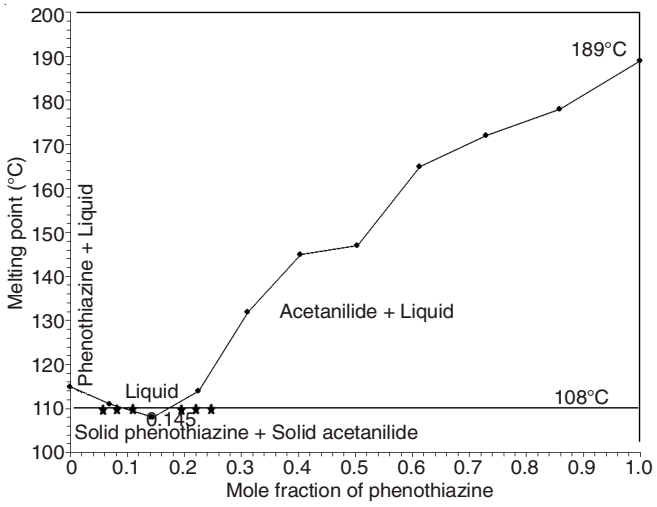

Fig. Phase diagram of phenothiazine-acetanilide system

Thermodynamic study: The values of heats of fusion of eutectic and non-eutectic are calculated by the mixture law. The value of heat of fusion of binary solid dispersions A_1-A_8 and E is reported in Table-1. The activity coefficient and activity of components for the systems under investigation has been calculated from the equation [14] given below:

$$-\ln\chi_i\gamma_i = \frac{\Delta H_i}{R}\left(\frac{1}{T_e} - \frac{1}{T_i}\right) \quad (1)$$

where χ_i, γ_i are mole fraction and activity coefficient of the component i in the liquid phase respectively. ΔH_i is the heat of fusion of component i at its melting point T_i and R is the gas constant. T_e is the melting temperature of alloy. Using the values of activity and activity coefficient of the components in the binary product, the mixing and excess thermodynamic functions have been evaluated.

Mixing functions: In order to know the mixing characteristics of components in the system; integral molar free energy of mixing (ΔG^M), molar entropy of mixing (ΔS^M) and molar enthalpy of mixing (ΔH^M) and partial thermodynamic mixing functions of the binary solid dispersions were determined by using the following equations:

$$\Delta G^M = RT\,(\chi_{PT} \ln a_{PT} + \chi_{ACT} \ln a_{ACT}) \quad (2)$$

$$\Delta S^M = -R\,(\chi_{PT} \ln \chi_{PT} + \chi_{ACT} \ln \chi_{ACT}) \quad (3)$$

$$\Delta H^M = RT\,(\chi_{PT} \ln \gamma_{PT} + \chi_{ACT} \ln \gamma_{ACT}) \quad (4)$$

$$G_i^M = \mu_i^M = RT \ln a_i \quad (5)$$

where G_i^M (μ_i^M) is the partial molar free energy of mixing of component i (mixing chemical potential)in binary mix and γ_i and a_i is the activity coefficient and activity of component respectively. The positive value [15] of molar free energy of mixing of alloys (Table-2) suggests that the mixing in all cases is non-spontaneous. The integral molar enthalpy of mixing value corresponds to the value of excess integral molar free energy of the system favours the regularity in the binary solutions.

Excess functions: In order to unfold the nature of the interactions between the components forming the eutectic and non-eutectic solid dispersions, the excess thermodynamic

TABLE-2
VALUE OF PARTIAL AND INTEGRAL MIXING OF GIBBS FREE ENERGY (ΔG^M), ENTHALPY (ΔH^M) AND ENTROPY (ΔS^M) OF PT-ACT SYSTEM

Alloy	ΔG_{PT}^{-M} (J/mol)	ΔG_{ACT}^{-M} (J/mol)	ΔG^M (J/mol)	ΔH_{PT}^{-M} (J/mol)	ΔH_{ACT}^{-M} (J/mol)	ΔH^M (J/mol)	ΔS_{PT}^{-M} (J/mol/K)	ΔS_{ACT}^{-M} (J/mol/K)	ΔS^M (J/mol/K)
A_1	-4332.21	-227.01	-514.71	4153.93	4.96	295.73	22.10	0.60	2.11
E	-4498.83	-397.27	-991.93	1618.29	98.90	319.18	16.06	1.30	3.44
A_2	-4165.58	-56.75	-982.15	630.69	764.28	734.20	12.39	2.12	4.43
A_3	-3165.84	964.79	-321.41	762.75	2220.98	1766.91	9.70	3.10	5.16
A_4	-2443.81	1702.58	26.81	704.66	3501.95	2371.42	7.53	4.30	5.61
A_5	-2332.73	1816.08	-276.23	57.65	4266.74	2144.03	5.69	5.83	5.76
A_6	-1332.99	2837.63	281.88	450.33	6292.76	2712.52	4.07	7.89	5.55
A_7	-944.20	3234.90	181.30	216.68	8088.45	2336.68	2.61	10.91	4.84
A_8	-610.95	3575.41	-21.70	-42.13	10927.38	1501.90	1.26	16.30	3.38

functions such as integral excess integral free energy (g^E), excess integral entropy (s^E) and excess integral enthalpy (h^E) were calculated using the following equations:

$$g^E = RT(\chi_{PT} \ln \gamma_{PT} + \chi_{ACT} \ln \gamma_{ACT}) \quad (6)$$

$$s^E = -R\left((\chi_{PT} \ln \gamma_{PT} + \chi_{ACT} \ln \gamma_{ACT} + \chi_{PT} T \frac{\delta \ln \gamma_{PT}}{\delta T} + \chi_{ACT} T \frac{\delta \ln \gamma_{ACT}}{\delta T} \right) \quad (7)$$

$$h^E = -RT^2 \left(\chi_{PT} \frac{\delta \ln \gamma_{PT}}{\delta T} + \chi_{ACT} \frac{\delta \ln \gamma_{ACT}}{\delta T} \right) \quad (8)$$

and excess chemical potential or excess partial free energy of mixing:

$$g_i^{-E} = \mu_i^{-M} = RT \ln \gamma_i \quad (9)$$

The values of $\delta \ln \gamma_i / \delta T$ can be determined by the slope of liquidus curve near the alloys. The values of the excess thermodynamic functions are given in Table-3. The value of excess free energy is a measure of the departure of the system from ideal behaviour. The reported excess thermodynamic data substantiate the earlier conclusion of an appreciable interaction between the parent components during the formation of alloys. The positive g^E value [16] for all eutectic and non-eutectic solid dispersions infers stronger interaction between like molecules in binary mixture. The excess entropy is a measure of the change in configurational energy due to a change in potential energy and indicates an increase in randomness.

Gibbs-Duhem equation: Further the partial molar quantity, activity and activity coefficient can also be determined by using Gibbs-Duhem equation [17]:

$$\sum \chi_i dz_i^{-M} = 0 \quad (10)$$

$$\text{or } \chi_{PT} dH_{PT}^{-M} + \chi_{ACT} dH_{ACT}^{-M} = 0 \quad (11)$$

$$\text{or } dH_{PT}^{-M} = \frac{\chi_{ACT}}{\chi_{PT}} dH_{ACT}^{-M} \quad (12)$$

$$\text{or } [H_{PT}^{-M}]_{x_{PT}=y} = \int_{\chi_{PT}=y}^{\chi_{PT}=1} \frac{\chi_{ACT}}{\chi_{PT}} dH_{ACT}^{-M} \quad (13)$$

Using eqn. 13, a graph between H_{ACT}^{-M} and χ_{ACT}/χ_{PT} gives the solution of the partial molar heat of mixing of a constituent phenothiazine in binary mix and plot between χ_{ACT}/χ_{PT} *vs.* ln a_{ACT} determines the value of activity of component phenothiazine in binary mix.

Stability function: Thermodynamic behaviour of the present system in form of stability and excess stability functions [18] can be determined by the second derivative of their molar free energy and excess energy respectively, with respect to the mole fraction of either constituent:

$$\text{Stability} = \frac{\partial^2 \Delta G^M}{\partial x^2} = -2RT \frac{\partial \ln a}{\partial (1-x)^2} \quad (14)$$

$$\text{Excess stability} = \frac{\partial^2 g^E}{\partial x^2} = -2RT \frac{\partial \ln \gamma}{\partial (1-x)^2} \quad (15)$$

These values were calculated by multiplying the slope of ln a *vs.* $(1 - x)^2$ and ln γ *vs.* $(1 - x)^2$ plots with -2RT. The best polynomial equation of the curve generated is given as:

$$\ln \gamma = 3.68\,(1-x)^2 - 21.44\,(1-x)^4 + 81.99\,(1-x)^6 - 146.84\,(1-x)^8 + 126.1\,(1-x)^{10} - 41.47\,(1-x)^{12} \quad (16)$$

The slope of the curve obtained by differentiating the above equation with respect to $(1 - x)^2$, which may also be used to calculate the excess stability of PT-ACT system. The values of total stability to ideal stability and defined as:

$$\text{Ideal stability} = \frac{RT}{x(1-x)} \quad (17)$$

These values showed that there is considerable thermodynamic stability in the alloy. Fig. 2 is for the stability, excess stability and ideal stability in the form of composition and partial Gibb's energy favours the formation of the binary alloys and their mixing.

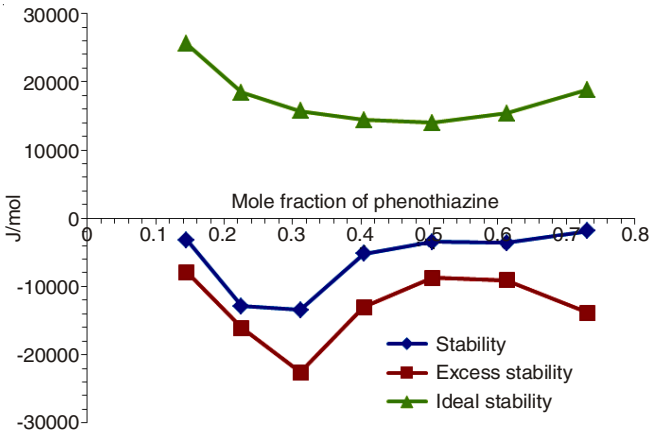

Fig. 2. Stability graph of phenothiazine-acetanilide system

Interfacial investigation

Solid-liquid interfacial energy (σ): Experimentally observed value of interfacial energy 'σ' has been reported with

TABLE-3
VALUE OF PARTIAL AND INTEGRAL EXCESS GIBBS FREE ENERGY (g^E), ENTHALPY (h^E) AND ENTROPY(s^E) OF PT-ACT SYSTEM

Alloy	g_{PT}^{-E} (J/mol)	g_{ACT}^{-E} (J/mol)	g^E (J/mol)	h_{PT}^{-E} (J/mol)	h_{ACT}^{-E} (J/mol)	h^E (J/mol)	s_{PT}^{-E} (J/mol/K)	s_{ACT}^{-E} (J/mol/K)	s^E (J/mol/K)
A_1	4153.93	4.96	295.73	149269.96	-8836.58	2243.88	377.91	-23.02	5.07
E	1618.29	98.90	319.18	390547.14	48555.80	98139.11	1020.81	127.18	256.75
A_2	630.69	764.28	734.20	29627.16	-5948.60	2063.79	74.93	-17.35	3.44
A_3	762.75	2220.98	1766.91	-3762.39	-12118.26	-9516.39	-11.17	-35.41	-27.86
A_4	704.66	3501.95	2371.42	82170.32	51118.68	63668.21	194.89	113.92	146.64
A_5	57.65	4266.74	2144.03	3420.78	7567.18	5476.08	8.01	7.86	7.93
A_6	450.33	6292.76	2712.52	367.93	19172.93	7649.23	-0.19	29.41	11.27
A_7	216.68	8088.45	2336.68	19404.11	100243.55	41175.51	43.12	207.09	87.28
A_8	-42.13	10927.38	1501.90	-74.73	134164.82	18820.33	-0.07	273.25	38.40

a variation of 50-100 % depending upon worker to worker. The solid-liquid interfacial energy (σ) calculated from melting enthalpy change by Singh and Glickman [19] was found in good agreement with the experimental values. Turnbull empirical relationship [20] between the interfacial energy and enthalpy change provides the clue to determine the interfacial energy value of binary solid dispersions and is expressed as:

$$\sigma = \frac{C\Delta H}{(N)^{1/3}(V_m)^{2/3}} \quad (18)$$

where the coefficient C lies between 0.33 to 0.35 for non-metallic system, V_m is molar volume and N is the Avogadro's constant. The value of the solid-liquid interfacial energy of phenothiazine and acetanilide was found to be 3.61×10^{-02} and 3.70×10^{-02} J m^{-2}, respectively and σ value of the solid dispersions was given in Table-1. The value of σ has also been determined by using the value of Gibbs-Thomson coefficient. The theoretical basis of determination of σ was made for equal thermal conductivities of solid and liquid phases for some transparent materials.

Gibbs-Thomson coefficient (τ): For a planar grain boundary on planar solid-liquid interface the Gibbs-Thomson coefficient (τ) for the system can be calculated by the Gibbs-Thomson equation and is expressed as:

$$\tau = r\Delta T = \frac{TV_m\sigma}{\Delta H} = \frac{\sigma}{\Delta S_V} \quad (19)$$

where τ is the Gibbs-Thomson coefficient, ΔT is the dispersion in equilibrium temperature and, r is the radius of grooves of interface. It was also determined by the help of Gunduz and Hunt numerical method [21] for materials having known grain boundary shape, temperature gradient in solid and the ratio of thermal conductivity of the equilibrated liquid phases to solid phase ($R = K_L/K_S$).The Gibbs-Thomson coefficient for phenothiazine, acetanilide and their solid dispersions are found in the range of $7.28–9.51 \times 10^{-06}$ Km and is reported in Table-1.

Interfacial grain boundary energy (σ_{gb}): Grain boundary is the internal surface which can be understood in a very similar way to nucleation on surfaces in liquid-solid transformation. In past, a numerical method [22] is applied to observe the interfacial grain boundary energy (σ_{gb}) without applying the temperature gradient for the grain boundary groove shape. For isotropic interface there is no difference in the value of interfacial tension and interfacial energy. A considerable force is employed at the grain boundary groove in anisotropic interface. The grain boundary energy can be obtained by the equation:

$$\sigma_{gb} = 2\sigma\cos\theta \quad (20)$$

where θ is equilibrium contact angle precipitates at solid-liquid interface of grain boundary. The grain boundary energy could be twice the solid-liquid interfacial energy in the case where the contact angle tends to zero. The value of σ_{gb} for solid phenothiazine and acetanilide was found to be 6.98×10^{-2} and 7.15×10^{-2} J m^{-2}, respectively and the value for all solid dispersions is given in Table-1.

Effective entropy change (ΔS_v): It is obvious that the effective entropy change and the volume fraction of phases in the alloy are inter-related to decide the interface morphology during solidification and the volume fraction of the two phases depends on the ratio of effective entropy change of the phases. The entropy of fusion ($\Delta S = \Delta H/T$) value (Table-1) of alloys is calculated by heat of fusion values of the materials. The effective entropy change per unit volume (ΔS_V) is given by:

$$\Delta S_V = \frac{\Delta H}{T}.\frac{1}{V_m} \quad (21)$$

where ΔH is the enthalpy change, T is the melting temperature and V_m is the molar volume of solid phase. The entropy of fusion per unit volume (ΔS_V) for phenothiazine and acetanilide was found 379 and 506 kJ K^{-1} m^{-3}, respectively. Values of ΔS_V for alloys are reported in Table-1.

Driving force of nucleation (ΔG_V): During growth of crystalline solid there is change in enthalpy, entropy and specific volume and non-equilibrium leads the Gibb's energy. Thermodynamically metastable phase occurs in a supersaturated or super-cooled liquid. The driving force for liquid-solid transition is the difference in Gibb's energy between the two phases. The theories of solidification process in past have been discussed on the basis of diffusion model, kinetic characteristics of nucleation and on thermodynamic features. The lateral motion of rudimentry steps in liquid advances stepwise with non-uniform surface at low driving force while continuous and uniform surface advances at sufficiently high driving force. The driving force of nucleation from liquid to solid during solidification (ΔG_V) can be determined at different undercoolings (ΔT) by using the following equation [23]:

$$\Delta G_V = \Delta S_V \Delta T \quad (22)$$

It is opposed by the increase in surface free energy due to creation of a new solid-liquid interface. By assuming that solid phase nucleates as small spherical cluster of radius arising due to random motion of atoms within liquid. The value of ΔG_V for each solid dispersions and pure components are given in the Table-4.

TABLE-4
VOLUME FREE ENERGY CHANGE (ΔG_v) DURING SOLIDIFICATION FOR PT-ACT SYSTEM OF DIFFERENT UNDERCOOLINGS (ΔT)

Alloy	ΔG_v (J/cm^3)					
	1.0	1.5	2.0	2.5	3.0	3.5
A_1	0.51	0.76	1.01	1.27	1.52	1.77
A_2	0.51	0.76	1.01	1.27	1.52	1.77
E	0.49	0.74	0.99	1.23	1.48	1.73
A_3	0.47	0.70	0.93	1.17	1.40	1.63
A_4	0.45	0.67	0.89	1.12	1.34	1.56
A_5	0.44	0.66	0.88	1.10	1.32	1.54
A_6	0.42	0.62	0.83	1.04	1.25	1.46
A_7	0.40	0.61	0.81	1.01	1.21	1.42
A_8	0.39	0.59	0.79	0.99	1.18	1.38
PT	0.38	0.57	0.76	0.95	1.14	1.33
ACT	0.51	0.76	1.01	1.27	1.52	1.77

Critical radius (r*): During liquid-solid transformation embryos are rapidly dispersed in unsaturated liquid and on undercooling liquid becomes saturated and provides embryo of a critical size with radius r* for nucleation which can be determined by the Chadwick relation [24]:

$$r^* = \frac{2\sigma}{\Delta G_V} = \frac{2\sigma T}{\Delta H_V \Delta T} \quad (23)$$

where σ is the interfacial energy and ΔH_V is the enthalpy of fusion of the compound per unit volume, respectively. The critical size of the nucleus for the components and alloys was calculated at different undercoolings and values are presented in Table-5. It can be inferred from table that the size of the critical nucleus decreases with increase in the undercooling of the melt. The existence of embryo and a range of embryo size can be expected in the liquid at any temperature. The value of r* for pure components (phenothiazine and acetanilide) and solid dispersions lies between 41 to 190 nm at undercooling 1-3.5 °C.

TABLE-5
CRITICAL SIZE OF NUCLEUS (r*) AT DIFFERENT UNDERCOOLINGS (ΔT)

Alloy	r* (nm)					
	1.0	1.5	2.0	2.5	3.0	3.5
A_1	145.7	97.12	72.84	58.27	48.56	41.62
A_2	145.6	97.08	72.81	58.25	48.54	41.60
E	149.1	99.37	74.53	59.62	49.69	42.59
A_3	157.3	104.85	78.63	62.91	52.42	44.93
A_4	163.7	109.14	81.85	65.48	54.57	46.77
A_5	166.0	110.65	82.99	66.39	55.33	47.42
A_6	174.7	116.49	87.37	69.89	58.25	49.92
A_7	179.3	119.54	89.66	71.72	59.77	51.23
A_8	183.7	122.44	91.83	73.46	61.22	52.47
PT	190.3	126.84	95.13	76.10	63.42	54.36
ACT	146.2	97.44	73.08	58.46	48.72	41.76

Critical free energy of nucleation (ΔG*): To form critical nucleus, it requires a localized activation/critical free energy of nucleation (ΔG*) which is evaluated [25] as:

$$\Delta G^* = \frac{16}{3}\frac{\pi\sigma^3}{\Delta G_v^2} \quad (24)$$

The value of ΔG* for alloys and pure components has been found in the range of 10^{-15} to 10^{-16} J per molecule at different undercoolings and has been reported in Table-6.

TABLE-6
CRITICAL FREE ENERGY OF NUCLEATION (ΔG*) FOR ALLOYS OF PT-ACT SYSTEM AT DIFFERENT UNDERCOOLING (ΔT)

Alloy	ΔG* × 10^{16} (J)					
	1.0	1.5	2.0	2.5	3.0	3.5
A_1	32.85	14.60	8.21	5.26	3.65	2.68
A_2	32.73	14.55	8.18	5.24	3.64	2.67
E	34.21	15.20	8.55	5.47	3.80	2.79
A_3	37.98	16.88	9.49	6.08	4.22	3.10
A_4	41.05	18.24	10.26	6.57	4.56	3.35
A_5	42.09	18.71	10.52	6.73	4.68	3.44
A_6	46.53	20.68	11.63	7.44	5.17	3.80
A_7	48.88	21.72	12.22	7.82	5.43	3.99
A_8	51.16	22.74	12.79	8.19	5.68	4.18
PT	54.78	24.35	13.69	8.76	6.09	4.47
ACT	33.15	14.74	8.29	5.30	3.68	2.71

Interface morphology: The science of growth has been developed on the foundation of thermodynamics, kinetics, fluid dynamics, crystal structures and interfacial sciences. The solid-liquid interface morphology can be predicted from the value of the entropy of fusion. According to Hunt and Jackson [26], the type of growth from a binary melt depends upon a factor α, defined as:

$$\alpha = \xi\frac{\Delta H}{RT} = \xi\frac{\Delta S}{R} \quad (25)$$

where ξ is a crystallographic factor depending upon the geometry of the molecules and has a value less than or equal to one. ΔS/R (also known as Jackson's roughness parameter α) is the entropy of fusion (dimensionless) and R is the gas constant. When α is less than two the solid-liquid interface is atomically rough and exhibits non-faceted growth. The value of Jackson's roughness parameter (α) is given in Table-1. For the entire solid dispersions the a value was found greater than 2 which indicate the faceted [27,28] growth proceeds in all the cases.

Conclusion

The solid-liquid equilibrium phase diagram of PT-ACT system shows the formation of simple eutectic alloy. The activity and activity coefficient values are very useful in computing thermodynamic mixing and excess functions. Thermodynamic excess and mixing functions g^E and ΔG^M values for eutectic and non-eutectics are being found positive which suggest the stronger association between like molecules and there is non-spontaneous mixing in all the binary drugs.

ACKNOWLEDGEMENTS

Thanks are due to The Head, Department of Chemistry, V.K.S. University, Ara, India for providing the research facilities.

REFERENCES

1. S.D. Srivastava and P. Kohli, *Proc. Nat. Acad. Sci. India*, **77**, 199 (2007).
2. W. Fang and T. Jie, *Acta Pharmacol. Sin.*, **24**, 1001 (2003).
3. A. Rajasekaran and P.P. Tripathi, *Acta Pharm. Turc.*, **45**, 235 (2003).
4. B.P. Kamat and J. Seetharamappa, *J. Pharm. Biomed. Anal.*, **35**, 655 (2004); http://dx.doi.org/10.1016/j.jpba.2004.02.008.
5. A.U. Gjerde, H. Holmsen and W. Nerdal, *Biochim. Biophys. Acta*, **1682**, 28 (2004); http://dx.doi.org/10.1016/j.bbalip.2004.01.004.
6. K. Dhirendra, S. Lewis, N. Udupa and K. Atin, *Pak. J. Pharm. Sci.*, **22**, 234 (2009).
7. A.O.L. Évora, R.A.E. Castro, T.M.R. Maria, M.T.S. Rosado, M. Ramos Silva, A.M. Beja, J. Canotilho and M.E.S. Eusébio, *Cryst. Growth Des.*, **11**, 4780 (2011); http://dx.doi.org/10.1021/cg200288b.
8. J.W. Rice and E.M. Suuberg, *J. Chem. Thermodyn.*, **42**, 1356 (2010); http://dx.doi.org/10.1016/j.jct.2010.05.019.
9. S. Dastidar, J. Kristiansen, J. Molnar and L. Amaral, *Antibiotics*, **2**, 58 (2013); http://dx.doi.org/10.3390/antibiotics2010058.
10. R. Sharma, P. Samadhiya, S.D. Srivastava and S.K. Srivastava, *J. Chem. Sci.*, **124**, 633 (2012); http://dx.doi.org/10.1007/s12039-012-0257-x.
11. J.S. Chickos, W.E. Acree and J.F. Liebman, *J. Phys. Chem. Ref. Data*, **28**, 1535 (1999); http://dx.doi.org/10.1063/1.556045.
12. J. Sangster, *J. Phys. Chem. Ref. Data*, **28**, 889 (1999); http://dx.doi.org/10.1063/1.556040.
13. A.K. Aggarwal and S. Jain, *Chem. Pharm. Bull. (Tokyo)*, **59**, 629 (2011); http://dx.doi.org/10.1248/cpb.59.629.
14. B.L. Sharma, S. Tandon and S. Gupta, *Cryst. Res. Technol.*, **44**, 258 (2009); http://dx.doi.org/10.1002/crat.200800034.
15. R. Malaviolle, G. De Maury, A. Chauvet, A. Terol and J. Masse, *Thermochim. Acta*, **121**, 283 (1987); http://dx.doi.org/10.1016/0040-6031(87)80179-X.

16. H. Shekhar and S.S. Salim, *Nat. Acad. Sci. Lett.*, **34**, 117 (2011).
17. P. Gupta, T. Agrawal, S.S. Das and N.B. Singh, *J. Chem. Thermodyn.*, **48**, 291 (2012); http://dx.doi.org/10.1016/j.jct.2012.01.001.
18. M. Shamsuddin, S.B. Singh and A. Nasar, *Thermochim. Acta*, **316**, 11 (1998); http://dx.doi.org/10.1016/S0040-6031(98)00291-3.
19. N.B. Singh and M.E. Glicksman, *J. Cryst. Growth*, **98**, 573 (1989); http://dx.doi.org/10.1016/0022-0248(89)90293-5.
20. D. Turnbull, *J. Chem. Phys.*, **18**, 768 (1950); http://dx.doi.org/10.1063/1.1747765.
21. M. Gunduz and J.D. Hunt, *Acta Metall.*, **37**, 1839 (1989); http://dx.doi.org/10.1016/0001-6160(89)90068-0.
22. S. Akbulut, Y. Ocak, K. Keslioglu and N. Marasli, *Appl. Surf. Sci.*, **255**, 3594 (2009); http://dx.doi.org/10.1016/j.apsusc.2008.10.003.
23. J.D. Hunt and S.Z. Lu, in ed.: D.T.J. Hurle, Hand Book of Crystal Growth, Elsevier, Amsterdam, p. 112 (1994).
24. G.A. Chadwick, Metallography of Phase Transformation, Butterworths, London, p. 61 (1972).
25. W.R. Wilcox, *J. Cryst. Growth*, **26**, 153 (1974); http://dx.doi.org/10.1016/0022-0248(74)90218-8.
26. J.D. Hunt and K.A. Jackson, *Trans. Metall. Soc. AIME*, **236**, 843 (1966).
27. H. Shekhar and V. Kant, *J. Indiam Chem. Soc.*, **88**, 947 (2011).
28. T. Agrawal, P. Gupta, S.S. Das, A. Gupta and N.B. Singh, *J. Chem. Eng. Data*, **55**, 4206 (2010); http://dx.doi.org/10.1021/je100358e.